Lutetium coating of nanoparticles by atomic layer deposition

Moret, Josette L.T.M.; Griffiths, Matthew B.E.; Frijns, Jeannine E.B.M.; Terpstra, Baukje E.; Wolterbeek, Hubert T.; Barry, Seán T.; Denkova, Antonia G.; Van Ommen, J. Ruud

DOI
10.1116/1.5134446

Publication date
2020

Document Version
Accepted author manuscript

Published in
Journal of Vacuum Science and Technology A: Vacuum, Surfaces and Films

Citation (APA)
Moret, J. L. T. M., Griffiths, M. B. E., Frijns, J. E. B. M., Terpstra, B. E., Wolterbeek, H. T., Barry, S. T., Denkova, A. G., & Van Ommen, J. R. (2020). Lutetium coating of nanoparticles by atomic layer deposition. *Journal of Vacuum Science and Technology A: Vacuum, Surfaces and Films*, *38*(2), Article 022414. https://doi.org/10.1116/1.5134446

Journal of Vacuum Science Technology A

Lutetium coating of nanoparticles by Atomic Layer Deposition

J.L.T.M. Moret[1,2], M.B.E. Griffiths[3], J.E.B.M. Frijns[2], B.E. Terpstra[1], H.T. Wolterbeek[1], S.T. Barry[3], A.G. Denkova[1], J.R. van Ommen[2]

[1] Applied Radiation and Isotopes, Applied sciences, Delft University of technology, Delft, the Netherlands

[2]Product and Process Engineering, Applied sciences, Delft University of technology, Delft, the Netherlands

[3]Department of Chemistry, Carleton University, Ottawa, Canada

Abstract

Atomic layer deposition (ALD) is a versatile gas phase coating technique that allows coating of complex structured materials, as well as high-surface area materials such as nanoparticles. In this work ALD is used to deposit a lutetium oxide layer on TiO_2 nano-particles (P25) in a fluidised bed reactor, to produce particles for nuclear medical applications. Two precursors were tested: the commercially available $Lu(TMHD)_3$ and the custom-made $Lu(HMDS)_3$. Using $Lu(TMHD)_3$ a lutetium loading up to 15 w% could be obtained, while $Lu(HMDS)_3$ only 0.16 w% Lu could be deposited due to decomposition of the precursor. Furthermore, it was observed that vibration-assisted fluidisation allows for better fluidisation of the nanoparticles and hence a higher degree of coating.

Keywords: Atomic layer deposition, Fluidised bed reactor, lutetium, lutetium acetylacetonate, lutetium tetra methyl heptadione, lutetium tris[bis(trimethylsilyl)amido)], titania p25, nuclear medical application

I. Introduction

Lutetium has various applications. For instance, lutetium oxide is used in semiconductor devices due to its favourable high dielectric constant [1, 2], as well as in catalysis because of its ability to reduce band gap energy and hence increase the catalytic effect [3]. In the field of nuclear medicine, lutetium – specifically the radioactive isotope ^{177}Lu – is one of the most promising therapeutic radionuclides due to its favourable decay characteristics [4, 5]. Upon radioactive decay, ^{177}Lu emits both a β^- particle and a gamma ray. The energy of the β^- particle (498 keV) is ideal for the treatment of (metastasised) tumours, while the gamma energy is suitable for imaging purposes, making ^{177}Lu a so-called theranostic (therapeutic *and* diagnostic) radionuclide. To ensure weekly patient treatment of various cancer types, hospitals are currently relying on weekly supplies of ^{177}Lu. However, hospitals prefer an 'on demand' supply to ensure patient treatment that is independent of suppliers. Radionuclide generators are ideal for this purpose, providing not only 'on demand' supply but usually also high specific activity (i.e. activity per unit mass), which is important to realise optimal therapeutic outcome [6]. A radionuclide generator typically consists of a material packed in a column holding the parent radioisotope. Upon radioactive decay of this parent radioisotope, a daughter radioisotope is formed. When eluting the radionuclide generator, the desired daughter radioisotope can be obtained, while the parent radioisotope remains on the column. In view of the extended use of ^{177}Lu, a radionuclide generator for this isotope is very much desired. However, the parent radionuclide ^{177m}Lu is chemically and physically identical to the daughter, so conventional separation techniques cannot be used. However, radiochemical properties can be exploited [5, 7]. In order to make use of these radiochemical properties, the parent radionuclide should be strongly immobilised, so that upon decay only the ^{177}Lu is released and can be extracted. This process has been previously demonstrated by Bhardwaj et al [7], indicating that the yield depends on the stability of the parent-substrate complex. Furthermore, this process is most efficient when the released ^{177}Lu can escape from its environment, therefore, thin lutetium nanostructures are beneficial.

If we were to build such a radionuclide generator, aiming at one patient dose (7.4 GBq [8]) per day, a coating of at least 32 w% Lu is required (Supplementary information S4) when considering an column elution efficiency of 80% and using 2 g of column material coated with natural occurring lutetium. To obtain this coating, atomic layer deposition (ALD) can be used. The advantage of using ALD is that a thin coating across the whole substrate can easily be fabricated due to the self-limiting behaviour of the process. Additionally, the amount of lutetium deposited can be tuned based on the application, as the lutetium content will depend on the number of cycles applied. In their 2012 review, Miikkulainen et al [9] reported three different Lu containing precursors used for ALD of lutetium-containing materials; namely $[Lu((Me_3Si)C_5H_4)_2Cl]_2$ [10], $Lu(^iPrO)_3$ [11], and $Lu[N(SiMe_3)_2]_3$ [12]. However, these precursors are not commercially available, which would be detrimental to practical implementation at a later stage. A fourth Lu-containing precursor, $Lu(TMHD)_3$, was reported by Roeckerath et al. [13]. This precursor is commercially available and was used in combination with a La containing compound to deposit the mixed-metal oxide $LaLuO_3$. The process is carried out in vacuum and, like with the other Lu precursors reported, Si-wafers were used as the substrate. Wafers have a small specific surface area in comparison to nanoparticles, which limits the amount that can be deposited. For the preparation of a radionuclide generator, nanoparticles having large surface area are necessary in order to achieve the desired Lu loading while still preserving the thin layer morphology.

The goal of this study is to deposit insoluble lutetium nanostructures on larger TiO_2 nanoparticle supports using a fluidised bed reactor (FBR). In an FBR, the substrate nanoparticles are suspended in a gas flow from below the reactor chamber, allowing the particles to behave as if they are a liquid. FBRs allow for scale-up of the coating process and permit good solid-gas mixing [14] and good heat transfer [15]. The applicability of lutetium tris(2,2,6,6-tetramethyl-3,5-heptanedionato) ($Lu(TMHD)_3$), lutetium tris hexamethyldisilazane ($Lu(HMDS)_3$), and lutetium tris acetylacetonate ($Lu(acac)_3$) in combination with the co-reactants O_3 and NH_3 is investigated in this paper.

Journal of Vacuum Science Technology A

II. Materials and methods

A. Chemicals

Lutetium tris(2,2,6,6-tetramethyl-3,5-heptanedionato) ($Lu(TMHD)_3$) was purchased from Strem chemicals (France). Lutetium trisacetylacetonate ($Lu(acac)_3$) was purchased from ABC Chemicals (Germany). Both substrates used in this study, silica (Aerosil 130) and titania (P25), were obtained from Evonik industries and dried overnight at 120°C before use. The carrier gas was 5.0 grade nitrogen. Ozone was produced with an ozone generator (Sanders C200) and synthetic air. NH_3 was obtained as mixture gas of 15w% NH_3 in N_2 from Linde gas. All precursors were transferred into custom-made stainless steel bubblers under inert conditions (nitrogen atmosphere). $LuCl_3$ was purchased from Strem Chemicals USA and used as received. Lithium bis(trimethylsilylamide) was purchased from Sigma-Aldrich chemical company and was used as received.

B. Preparation of $Lu(HMDS)_3$

$Lu(HMDS)_3$ was prepared according to Bradley et al. [16] Under inert conditions lithium bis(trimethylsilylamide) was dissolved in tetrahydrofuran and cooled. To this mixture $LuCl_3$ was added and after 24 h stirring at room temperature all solvent was removed under vacuum. The compound was then extracted to n-pentane and recrystalised three times before being purified by sublimation.

C. Thermogravimetric analysis

TGA measurements were performed using a Mettler Toledo TGA apparatus. A temperature sweep from 20 °C to 800 °C was undertaken with a heating rate of 10 °C/min in a nitrogen flow of 0.1 l/min.

Additional TGA measurements were performed using a National instruments TGA instrument, under inert loading conditions. The temperature sweep was from 20 °C to 600 °C with a heating rate of 10 °C/min in a nitrogen flow of 0.06 l/min.

D. Coating

Atomic layer deposition (ALD) was performed in a custom-made fluidised bed reactor (Figure 1). The fluidised bed reactor consisted of a glass column with an internal diameter of 25 mm and a length of 500 mm mounted on a stainless steel windbox with a stainless-steel distributer plate. On top of the column a distributer plate and a metal chamber were also connected. The required dosing time for $Lu(TMHD)_3$ was calculated to be 23 minutes and $Lu(HMDS)_3$ to be 10 minutes. For the co-reactants O_3 and NH_3 the dosing times were calculated to be 1.62 minutes and 2 minutes, respectively. The precursor and co-reactant were alternatively fed into the reactor chamber from the bottom of the reactor using nitrogen as a carrier gas, separated by 10 minute purge pulses. The carrier gas flow was 0.5 l/min ($1.52 * 10^{-2}$ m/s). During the purge an additional nitrogen flow of 0.1 l/min ($0.30 * 10^{-2}$ m/s) was added. The lutetium precursor was kept in a custom-made stainless-steel bubbler heated with heating tape and was transported to the reaction chamber through heated stainless-steel tubing. The fluidised bed was heated using an infra-red lamp. The whole system was controlled using a PC with a custom made Labview program. The off gasses were washed with a series of wash bottles containing acidic water and kaydol oil and then an active carbon/HEPA filter.

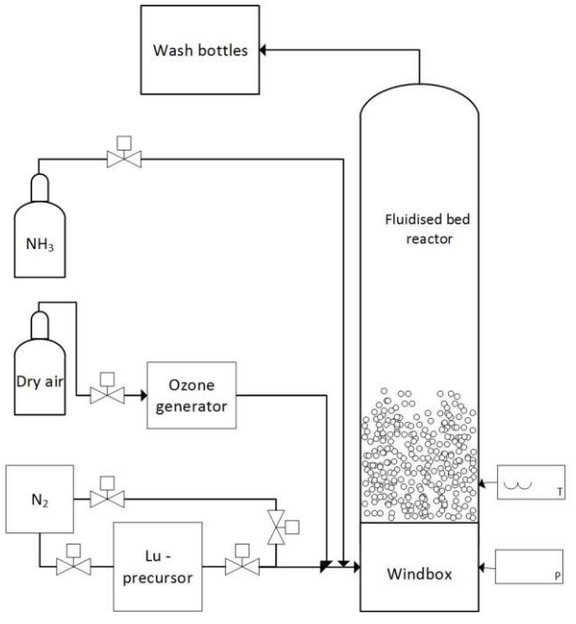

Figure 1: Schematic representation of the fluidised bed reactor setup.

E. Particle Analysis

The lutetium content of the obtained particles was determined using instrumental neutron activation analysis (INAA) at the Reactor institute Delft. For this purpose, the particles were irradiated with a thermal neutron flux of $5*10^{16}$ n /s m^2, epithermal neutral flux of $9*10^{14}$ n/s m², and a fast neutron flux of $3.6*10^{15}$ n/s m² for 5 minutes. Using the obtained lutetium mass fraction, the layer thickness can be determined according to Valdesueiro et al. [17]:

$$\delta = \frac{\sqrt[3]{\frac{6}{\pi} \cdot V_{Lu_2O_3}^{1p} + d_{3,2}^3} - d_{3,2}}{2}$$

with

$$V_{Lu_2O_3}^{1p} = \frac{x_{Lu}}{1 - \frac{M_{Lu_2O_3}}{2M_{Lu}} \cdot x_{Lu}} \cdot \frac{M_{Lu_2O_3}}{2M_{Lu}} \cdot \frac{\rho_{TiO_2}}{\rho_{Lu_2O_3}} \cdot \frac{\pi}{6} \cdot d_{3,2}^3$$

using a particle diameter of $d_{3,2}$ = 32.7 nm and density of 4200 kg/m³ [18]. The density of Lu_2O_3 as deposited was assumed to be 9420 kg/m³ [19]. Dividing the layer thickness by the number of cycles gives the growth per cycle (GPC). Transmission electron microscopy (TEM) and scanning electron microscopy-electron dispersive spectroscopy (SEM-EDS, Jeol) were used to image the coating. The chemical environment of the deposited lutetium was characterised using X-ray photoelectron spectroscopy (XPS).

III. Results and discussion

A. Precursor and co-reactant selection

The three potential precursors, $Lu(acac)_3$, $Lu(TMHD)_3$ and $Lu(HMDS)_3$, were first characterized using thermogravimetric analysis (TGA) to determine their applicability as ALD precursors. These TGA measurements were also used to calculate the vapour pressure of the compounds [20]. Considering the sensitivity of the precursors to air and moisture, measurements were carried in air as well as under a

nitrogen atmosphere. Figure 2 shows indeed that air has a strong influence on the stability of the precursors. $Lu(HMDS)_3$ loaded under inert conditions shows a smooth mass loss curve during the analysis, while the same measurement in air resulted in low mass loss and a high residual mass.

A suitable precursor should have one single mass loss over the temperature range tested with virtually no remaining mass [21]. Therefore, based on these criteria, $Lu(THMD)_3$ is the most suitable precursor from the candidates tested, with a single mass loss starting at 190°C and virtually no mass remaining. However, even though $Lu(HMDS)_3$ has about 20% residual mass, it shows potential if kept under inert conditions, because of its single mass loss starting at 110°C. The advantage of using $Lu(HMDS)_3$ over $Lu(THMD)_3$ is that $Lu(HMDS)_3$ can be used to deposit lutetium at lower temperatures. $Lu(acac)_3$, on the other hand, showed a stepwise mass loss, the first mass loss is between 280 °C and 400°C with the most significant mass loss at 310°C. The second mass loss is between 800°C and 850°C with around 80% of the initial mass remaining, indicating that the compound decomposes when heated. Therefore, $Lu(acac)_3$ was determined to be unsuitable to use as an ALD precursor (Figure 2).

Selection of a co-reagent for deposition of a lutetium containing film requires the ability to oxidise the precursor on the surface of the substrate. Initially, ozone was considered as a co-reagent because it is known for its strong oxidising potential. However, when an in water insoluble Lu layer is required a different co-reactant is needed. Lutetium is able to form several insoluble compounds like LuF and LuN [22]. Although HF is reported by Miikkulainen et al. [9] to make fluorides, it is strongly corrosive to the experimental setup and requires extra care when handled in the lab. Therefore, deposition of the nitride was preferred over the fluoride. The first experiments were carried out with ozone as co-reactant, as ozone was readily available.

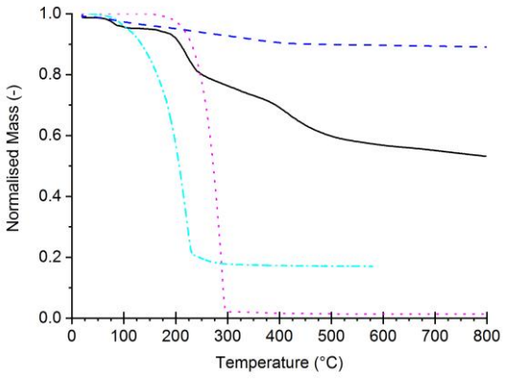

Figure 2: Thermogravimetric analysis using nitrogen as carrier gas of $Lu(acac)_3$ [——], $Lu(TMHD)_3$ [·····], $Lu(HMDS)_3$ [- - - -] exposed to air during loading and $Lu(HMDS)_3$ [- - -] loaded under inert conditions.

B. Lutetium deposition

1. *$Lu(TMHD)_3$ with O_3*

The dosing time for $Lu(TMHD)_3$ was determined by calculating the dosing time for a single cycle based on the vapour pressure of $Lu(TMHD)_3$ at 210°C (P_{vap}=42.7 Pa). (See section S1 in the supplementary information for vapour pressure calculation and section S2 for dose time calculation.) These calculated dosing times were taken as the base case: 23 minutes of $Lu(THMD)_3$ and 0.81 min O_3 for 1.3 g titania P25 as the substrate. Titania P25 was chosen as substrate for its strong metal-substrate interactions [23]. The expected Lu deposition for one cycle is 1.5w%. The precursor pulses were separated by 10-minute purge pulses. Then several experiments with dosing times deviating from these times were conducted in order to determine if there is self-limiting behaviour. The lutetium loading on the particles was determined using INAA. The measurement uncertainty in the INAA measurements range from 2 to 4 % (Figure 3).

The first observation during the experiments is, due to the low mass of the nano-particle agglomerates, some of the substrate material was sticking to the top of the column and reducing the bed volume, which might have led to earlier saturation. Tapping the column caused this cake to break down and fall back into the fluidised bed. Alternatively, the cake could be broken down by a

small back pulse of nitrogen after every cycle. This caking could have an influence on the coating applied. As the cake was not fluidising, a limited surface area was then exposed to the gas flow and could be coated. The influence on the lutetium loading of the particles in the bed was minimal, as we found that the cake had a comparable Lu loading to the particles in the bed.

Secondly, the coating process is delicate. Because of the relatively high precursor temperature, heat sinks could easily occur in the setup, even with extensive insulation. These heat sinks caused condensation of the precursor compound, leading to blockage of the system, which in turn reduced the nitrogen carrier gas flow and therefore the amount of Lu deposited. Also, large heat sinks in the wind box were sometimes observed. This resulted in large deposition of precursor in the windbox (Fig. S3). On the other hand, hot spots in the bubbler caused by inhomogeneous heating of the bubbler could give unexpectedly high Lu loading on the particles. During the experiments a temperature difference up to 40 °C between the front and back of the bubbler was observed. Furthermore, during the experiments it became clear that the state of the $Lu(TMHD)_3$ was influenced by its residence time in the heated bubbler. Upon refilling of the bubbler, it was observed that the remaining precursor had changed colour (from white to pale yellow), indicating some amount of decomposition. During the initial TGA this was not noticed because the decomposition is a rather slow process compared to evaporation. An additional TGA of the $Lu(TMHD)_3$ precursor that was heated up and cooled down showed that its temperature response had changed and some mass remained (Fig. S2), indicating decomposition.

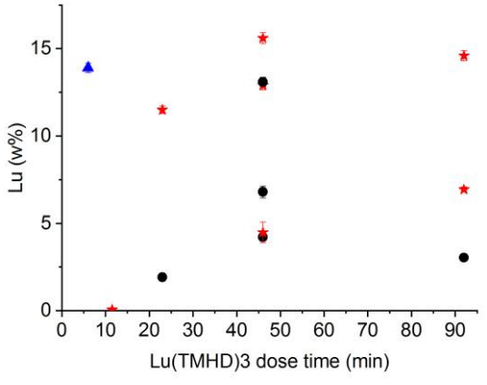

Figure 3: Lu weight fraction (Lu (w%)) versus the dosing time of $Lu(TMHD)_3$. Precursor temperature was 210°C, reactor temperature was 230°C and 4 cycles were applied using O_3 as co-reactant. Red stars are obtained with vibration assisted fluidisation while black rounds refer to non-vibration assisted fluidisation. The blue triangle is an experiment were 25 cycles were applied. Error bars represent the measurement uncertainty of INAA. Because of the spread in results, it was chosen to report the individual experiments rather than the average.

Figure 3 shows the deposition of lutetium as function of the exposure time to $Lu(TMHD)_3$. It seems that for the experiments of 46 min and longer, self-limiting behaviour occurs, as the amount of lutetium deposited goes to an asymptotic value, but the required long dosing times limited the number of experiments we could carry out. Typically, vibration assistance led to higher Lu loading. Vibration assistance allows for more efficient fluidisation compared to non-vibration assisted fluidisation as it leads to effective breaking of inter particle forces [24]. This means that more bare surface area of the particles is exposed to the precursor, explaining the difference in Lu loading in both regimes. The corresponding growth per cycle (GPC) ranges from about 0.03 nm to about 0.11 nm. Compared to other lutetium ALD processes this GPC is relatively low [12]. Nevertheless, it should be noted that those processes were operated under vacuum and using a different precursor, therefore they are not directly comparable to the process described here. However, GPCs reported for other lanthanide $(TMHD)_3$ ALD processes [25] are comparable or are much lower [26]. The large deviation in the data can also be caused by the low vapour pressure of the precursor in combination with the gas flow rate. Possibly the vapour above the precursor in the bubbler cannot saturate the headspace quickly enough during a pulse cycle, resulting in a decrease in precursor concentration over the duration of the Lu pulse. Keeping this in mind, the Lu precursor pulse was reduced to 6 minutes, while the number of cycles was increased (Blue triangle in Figure 3). The accumulated $Lu(TMHD)_3$ dose then was comparable to 3 cycles of 46 minutes. The deposited amount of Lu for the 25 cycles at 6 minutes per cycle was similar to the deposition for the 4 cycles at 46 minutes per cycle. Even though the accumulated $Lu(TMHD)_3$ pulse was shorter, the lutetium deposited was higher, which suggests that more and shorter pulses is indeed more effective for this low vapour pressure precursor. Furthermore, the GPC (Figure 6) seemed to decrease when the number of cycles was

increased. We attributed this mainly to the TiO_2 having more active surface sites for chemisorption than the overlayers of Lu_2O_3. The first reaction deposits more Lu when $Lu(TMHD)_3$ reacts with TiO_2 surfaces than subsequent reactions where $Lu(TMHD)_3$ reacts with Lu_2O_3 surfaces [27-29]. This might also be due to decomposition of the precursor during use, since increasing the number of cycles resulted in exposing the precursor to high temperature over a prolonged period of time.

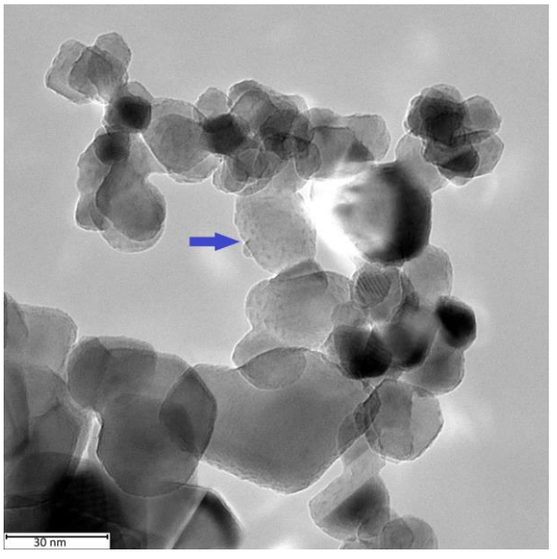

Figure 4: TEM image of the coated particles. 46 min dose time of $Lu(TMHD)_3$ per cycle and 4 cycles, loading 13 w% Lu. Arrow indicates possible island formation.

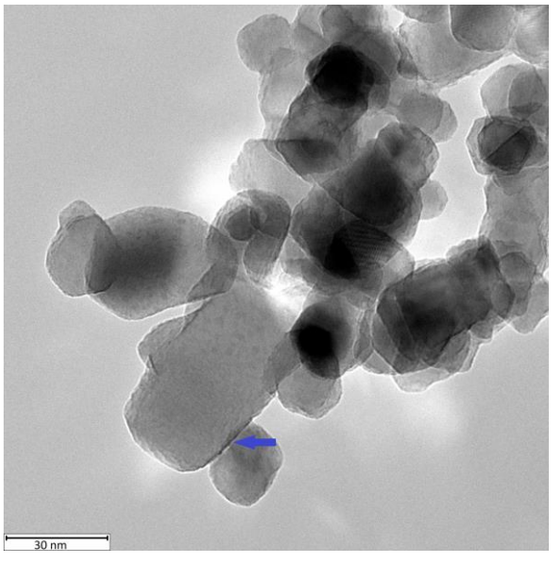

Figure 5: TEM images of coated particles. 6 min dose time of $Lu(TMHD)_3$ per cycle and 25 cycles, loading 14 w% Lu. The arrow indicates the deposited film.

The lutetium coating can be visualised using transmission electron microscopy (TEM), however it is very difficult to get an accurate visualisation of the coating within the 2 nm resolution or drawn any hard conclusions. Because lutetium is a heavy element, it should appear darker in the image compared to the titania substrate. Using TEM, the layer thickness was estimated to be 0.75 nm and is therefore not comparable to the calculated layer thickness based on the INAA measurements (0.12 nm). However, the calculations are based on the assumption that a uniform layer is achieved. Due to agglomeration, it is possible that at some places a thicker coat resulted, while at other places no film was formed. As well, the dose time seems to have an influence on the layer growth. While 4 cycles at 46 min per cycle resulted in mainly island growth (see arrow Figure 4), 25 cycles at 6 min per cycle resulted in mainly film growth (see arrow Figure 5). This may be due to the preferential chemisorption or decomposition of the precursor at newly-nucleated Lu sites: in a long pulse, decomposition carried on with precursor being continually supplied, where with short pulses, once the oxide formed, decomposition of the precursor was less likely.

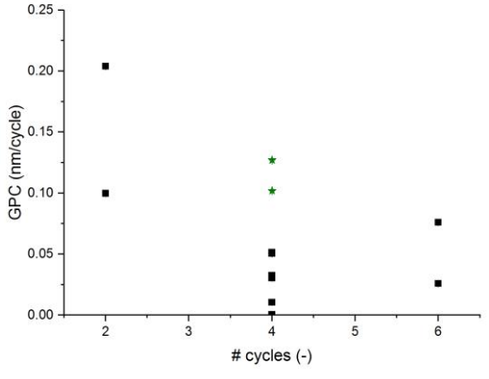

Figure 6: Growth per cycle (GPC) for precursor pulses $Lu(TMHD)_3$ and O_3 46 min and 1.6 min, respectively. The layer thickness is derived from the amount of lutetium deposited determined by INAA. The squares are non-vibration assisted, while the stars are vibration assisted. Because of the wide spread in results, it was chosen to report the individual experiments rather than the average.

2. *Lu(TMHD)$_3$ and NH$_3$*

For the application of the Lu-support particles in a radionuclide generator, an insoluble lutetium containing layer is needed. LuN is reported to be insoluble in water [22]. Using NH_3 as a co-reactant it is possible to deposit such a coating [9]. Therefore, coating experiments using $Lu(TMHD)_3$ and NH_3 were conducted. The Lu coating results are given in Figure 7. The Lu deposition is comparable to the coating results using ozone as co-reactant and again there was a large spread in the amount of lutetium that is deposited, which is again due to the varying fluidization conditions.

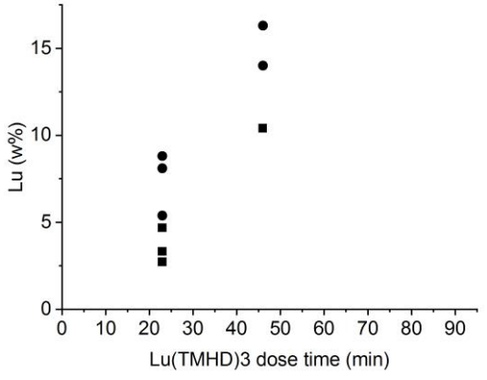

Figure 7: Lu loading (Lu (w%)) as function of precursor dosing time using $Lu(TMHD)_3$ and NH_3. The circles represent a NH_3 pulse of 10 min while the squares represents a NH_3 pulse of 1 min. Precursor temperature was 210°C, deposition temperature was 230°C, and 4 cycles were applied. The Lu loading was determined by INAA. Because of the wide spread in results, it was chosen to report the individual experiments rather than the average.

In order to determine the deposition of N on the particles, X-ray photoelectron spectroscopy (XPS) measurements were performed on the coated particles. Unfortunately, no N was detected on the particles. Firstly, it was assumed that the amount of N on the particles was too small to be detected, indicating that the amount of NH_3 supplied to the reaction chamber was too low. However, a tenfold increase in the NH_3 pulse still resulted in no N present on the coated particles. This could indicate that the concentration of NH_3 in the co-reactant feed it too low (i.e. a conservative concentration was chosen for safety reasons) or that undesired reactions are taking place (i.e. decomposition of NH_3). M. Guarino et al [30] reported that TiO_2 is used to reduce NH_3 concentrations in gas flows. This

could mean that NH_3 is decomposed at the substrates surface instead of oxidising the precursor molecules. Future research in our group will be aimed at investigating whether further increasing the NH_3 concentration does clearly lead to LuN deposition.

3. *Lu(HMDS)$_3$ and O$_3$*

The second precursor that showed potential in the TGA characterization was $Lu(HMDS)_3$. The advantage of using $Lu(HMDS)_3$ over $Lu(TMHD)_3$ is that the coating process can be undertaken at a lower bubbler temperature (130°C instead of 210°C). However, $Lu(HMDS)_3$ is more sensitive to oxygen and moisture. Based on the calculated vapour pressure of $Lu(HMDS)_3$ (P_{vap}=130 Pa, For calculation see section S1 in the Supplementary Information) and the same assumptions made for the coating as with $Lu(THMD)_3$ the dosing times for a full monolayer are a 10 minute pulse of $Lu(HMDS)_3$ and a 0.81 minute pulse of O_3 separated by 10 minute purge pulses. These dosing times were taken as the base case. Again, experiments with other pulse times were conducted to prove self-limiting behaviour. The Lu deposition was determined via neutron activation analysis (INAA). For these measurements the measurement uncertainty was 2 to 7%.

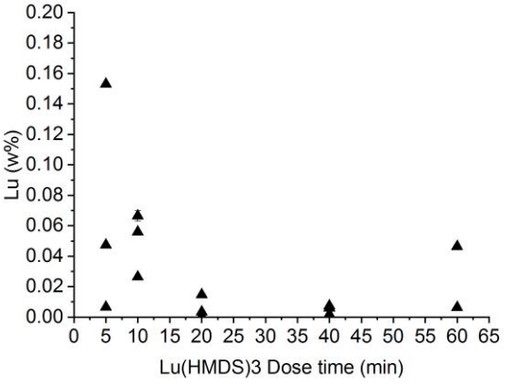

Figure 8: Lu deposition (Lu (w%)) as function of the precursor dosing time for $Lu(HMDS)_3$ as precursor and ozone co-reactant. Precursor temperature was kept at 130°C while the reactor temperature was at 200°C. 4 cycles were applied. Lu deposition was determined by INAA. Because of the wide spread in results, it was chosen to report the individual experiments rather than the average.

Figure 8 shows that the Lu deposition using $Lu(HMDS)_3$ is much lower compared to $Lu(TMHD)_3$. The most likely explanation for these results is that the precursor decomposed during operation. This possibility was supported by visual inspection of the bubbler showing that the $Lu(HMDS)_3$ precursor had changed colour from white to a pale yellow. In addition, the experiment conducted with a freshly filled bubbler showed the higher Lu deposition compared to experiments conducted thereafter.

In previous research by G. Scarel et al. [12] using $Lu(HMDS)_3$ as precursor growth rates up to 0.5 nm/cycle were obtained. The growth rate of our experiments was at least three orders of magnitude lower. It must be noted that Scarel's experiments were conducted on wafers while our experiments were performed on particles. The order of magnitude change in surface area can have an influence on the deposition rate.

Furthermore, as the TGA already indicated, $Lu(HMDS)_3$ decomposes when in contact with air and moisture as well as when heated up to elevated temperatures. Even though the bubbler was operated at relatively low temperature, prolonged exposure to elevated temperature led to decomposition of the precursor. All in all, $Lu(HMDS)_3$ seems less attractive to be used as ALD precursor than $Lu(THMD)_3$.

IV. Conclusions

We have shown that atomic layer deposition of lutetium is possible at atmospheric pressure using a fluidised bed reactor. The amount of lutetium strongly depends on the precursor chosen. Even though TGA measurements indicated two potential precursors ($Lu(HMDS)_3$ and $Lu(TMHD)_3$), only the latter gave a significant amount of lutetium deposition. Furthermore, proper fluidisation of the bed has a strong influence on the amount of Lu deposited on the particles. Also, reproducibility of the system is low. Future research will aim at increased and more constant deposition of Lutetium on particles for use in a radionuclide generator.

Funding:

This work is part of a project funded by NWO and IDB-Holland b.v. under project number 13306.

Acknowledgements:

H. Van Bui and D. LaZara are thanked for making the TEM-images. F. Hashemi is thanked for the XPS measurements. M. Talebi and A. Goulas are thanked for their help with ALD system trouble shoot. B. Boshuizen is thanked for updating the Labview program and B. Van der Linden is thanked for assisting with the TGA measurements at TU Delft. R. van den Heuvel is thanked for the calibration data of the TGA machine at TU Delft. B.E. Terpstra and M. Sarilar are thanked for the INAA analysis.

Author contribution: Investigation: JM, JF, MG, Elemental analysis: BT, Writing – original draft: JM, Writing – review and editing: SB, AD, RvO, Supervision: SB, HW, RvO, AD

References

[1]P. Darmawan, M. Y. Chan, T. Zhang, Y. Setiawan, H. L. Seng, T. K. Chan, T. Osipowicz and P. S. Lee, Appl Phys Lett **93** (6), 062901 (2008). https://doi.org/10.1063/1.2970036
[2]P. Darmawan, P. S. Lee, Y. Setiawan, J. Ma and T. Osipowicz, Appl Phys Lett **91** (9), 092903 (2007). https://doi.org/10.1063/1.2771065
[3]D. Wu, C. Li, Q. Kong, Z. Shi, D. Zhang, L. Wang, L. Han, X. Zhang and Q. Lin, J Rare Earths **36** (8), 819-825 (2018). https://doi.org/10.1016/j.jre.2018.01.016
[4]M. R. A. Pillai, S. Chakraborty, T. Das, M. Venkatesh and N. Ramamoorthy, Appl Radiat Isotopes **59** (2–3), 109-118 (2003). https://doi.org/http://dx.doi.org/10.1016/S0969-8043(03)00158-1
[5]D. J. De Vries and H. T. Wolterbeek, Tijdschr Nucl Geneesk **34** (2), 899-904 (2012).
[6]World Nuclear Association, http://www.world-nuclear.org/info/non-power-nuclear-applications/radioisotopes/radioisotopes-in-medicine/, Accesed on 24 february 2015
[7]R. Bhardwaj, A. van der Meer, S. K. Das, M. de Bruin, J. Gascon, H. T. Wolterbeek, A. G. Denkova and P. Serra-Crespo, Sci Rep **7**, 44242 (2017). https://doi.org/10.1038/srep44242
[8]European Medicine Agency, 'Lutathera, INN-lutetium(177Lu)oxodetreotide - Annex I', EPAR (2018).
[9]V. Miikkulainen, M. Leskelä, M. Ritala and R. L. Puurunen, Appl Phys Rev **113** (021301) (2013).
[10]G. Scarel, E. Bonera, C. Wiemer, G. Tallarida, S. Spiga, M. Fanciulli, I. L. Fedushkin, H. Schumann, Y. Lebedinskii and A. Zenkevich, Appl Phys Lett **85** (4), 630 (2004). https://doi.org/10.1063/1.1773360
[11]H. L. Lu, G. Scarel, L. Lamagna, M. Fanciulli, S.-J. Ding and D. W. Zhang, Appl Phys Lett **93** (15), 152906 (2008). https://doi.org/10.1063/1.3002373
[12]G. Scarel, C. Wiemer, G. Tallarida, S. Spiga, G. Seguini, E. Bonera, M. Fanciulli, Y. Lebedinskii, A. Zenkevich, G. Pavia, I. L. Fedushkin, G. K. Fukin and G. A. Domrachev, J Electrochem Soc **153** (11), F271 (2006). https://doi.org/10.1149/1.2347109
[13]M. Roeckerath, T. Heeg, J. M. J. Lopes, J. Schubert, S. Mantl, A. Besmehn, P. Myllymäki and L. Niinistö, Thin Solid Films **517** (1), 201-203 (2008). https://doi.org/10.1016/j.tsf.2008.08.064

[14]D. Kunii and O. Levenspiel, *Fluidization engineering*. (Elsevier, 2013).
[15]A. W. Weimer, in *Carbide, Nitride and Boride Materials Synthesis and Processing*, edited by A. W. Weimer (Springer Netherlands, Dordrecht, 1997), pp. 169-180.
[16]D. C. Bradley, J. S. Ghotra and F. A. Hart, J Chem Soc, Dalton T (10), 1021-1023 (1973). https://doi.org/10.1039/DT9730001021
[17]D. Valdesueiro, G. Meesters, M. Kreutzer and J. R. van Ommen, Materials **8** (3), 1249-1263 (2015).
[18]Evonik Industries, 'Basic characteristics of AEROSIL fumed silica'.
[19]Cas Solutions, www.scifinder.cas.org, Accesed on 15 March 2016
[20]D. M. Price, Thermochim Acta **367-368**, 253 (2000). https://doi.org/0040-6031/01/$
[21]S. Barry, presented at the ALD 2016, Dublin, Ireland, 2016 (unpublished).
[22]*CRC handbook of Chemistry and Physics*, edited by J. R. Rumble (CRC press, 88th edition).
[23]J. S. Tauster, S. C. Fung and R. L. Garten, J am chem soc **100** (1), 170 (1978).
[24]S. W. Park, J. Woo Kim, H. Jong Choi and J. Hyung Shim, J Vac Sci Technol A **32** (1), 01A115 (2014). https://doi.org/10.1116/1.4845735
[25]J. Päiväsaari, M. Putkonen and L. Niinistö, Thin Solid Films **472** (1-2), 275-281 (2005). https://doi.org/10.1016/j.tsf.2004.06.160
[26]T. Boekhoudt, Master thesis, Technische Universiteit Delft, 2016.
[27]R. L. Puurunen, Chem Vapor Depos **9** (5), 249-258 (2003). https://doi.org/10.1002/cvde.200306265
[28]R. L. Puurunen, J of Appl Phys **97** (12), 121301 (2005). https://doi.org/10.1063/1.1940727
[29]R. L. Puurunen and W. Vandervorst, J Appl Phys **96** (12), 7686-7695 (2004). https://doi.org/10.1063/1.1810193
[30]M. Guarino, A. Costa and M. Porro, Bioresour Technol **99** (7), 2650-2658 (2008). https://doi.org/10.1016/j.biortech.2007.04.025

Figure captions

Figure 1: Schematic representation of the fluidised bed reactor setup.
Figure 2: Thermogravimetric analysis using nitrogen as carrier gas of $Lu(acac)_3$ [ ], $Lu(TMHD)_3$ [ ], $Lu(HMDS)_3$ [ ] exposed to air during loading and $Lu(HMDS)_3$ [ ] loaded under inert conditions.
Figure 3: Lu weight fraction (Lu (w%)) versus the dosing time of $Lu(TMHD)_3$. Precursor temperature was 210°C, reactor temperature was 230°C and 4 cycles were applied using O_3 as co-reactant. Red stars are obtained with vibration assisted fluidisation while black rounds refer to non-vibration assisted fluidisation. The blue triangle is an experiment were 25 cycles were applied. Error bars represent the measurement uncertainty of INAA. Because of the spread in results, it was chosen to report the individual experiments rather than the average.
Figure 4: TEM image of the coated particles. 46 min dose time of $Lu(TMHD)_3$ per cycle and 4 cycles, loading 13 w% Lu. Arrow indicates possible island formation.
Figure 5: TEM images of coated particles. 6 min dose time of $Lu(TMHD)_3$ per cycle and 25 cycles, loading 14 w% Lu. The arrow indicates the deposited film.
Figure 6: Growth per cycle (GPC) for precursor pulses $Lu(TMHD)_3$ and O_3 46 min and 1.6 min, respectively. The layer thickness is derived from the amount of lutetium deposited determined by INAA. The squares are non-vibration assisted, while the stars are vibration assisted. Because of the wide spread in results, it was chosen to report the individual experiments rather than the average.

Journal of Vacuum Science Technology A

Figure 7: Lu loading (Lu (w%)) as function of precursor dosing time using $Lu(TMHD)_3$ and NH_3. The circles represent a NH_3 pulse of 10 min while the squares represents a NH_3 pulse of 1 min. Precursor temperature was 210°C, deposition temperature was 230°C, and 4 cycles were applied. The Lu loading was determined by INAA. Because of the wide spread in results, it was chosen to report the individual experiments rather than the average.

Figure 8: Lu deposition (Lu (w%)) as function of the precursor dosing time for $Lu(HMDS)_3$ as precursor and ozone co-reactant. Precursor temperature was kept at 130°C while the reactor temperature was at 200°C. 4 cycles were applied. Lu deposition was determined by INAA. Because of the wide spread in results, it was chosen to report the individual experiments rather than the average.

Journal of Vacuum Science Technology A

PLEASE CITE THIS ARTICLE AS DOI: 10.1116/1.5134446

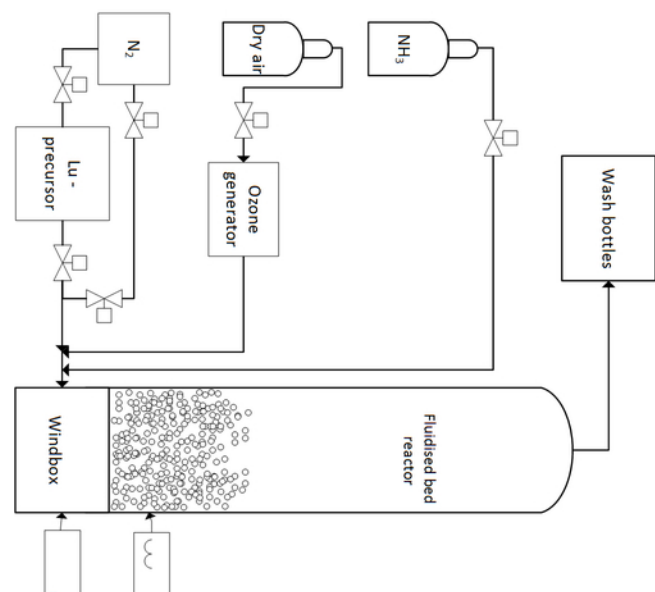

Journal of Vacuum Science Technology A

PLEASE CITE THIS ARTICLE AS DOI: 10.1116/1.5134446

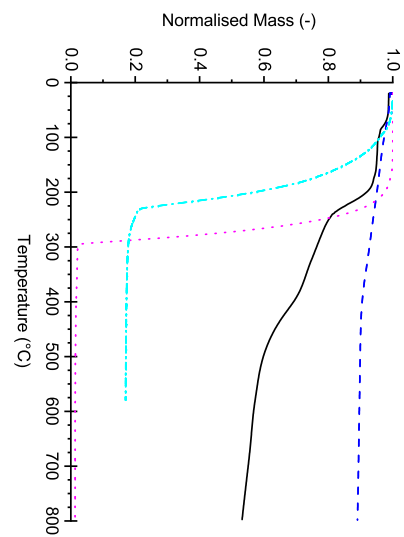

Journal of Vacuum Science Technology A

PLEASE CITE THIS ARTICLE AS DOI: 10.1116/1.5134446

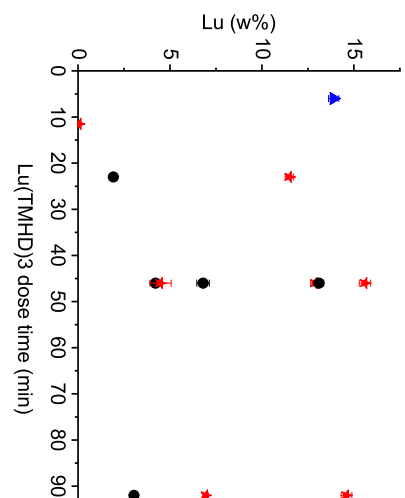

Journal of Vacuum Science Technology A

ACCEPTED MANUSCRIPT

PLEASE CITE THIS ARTICLE AS DOI: 10.1116/1.5134446

Journal of Vacuum Science Technology A

ACCEPTED MANUSCRIPT

PLEASE CITE THIS ARTICLE AS DOI: 10.1116/1.5134446

Journal of Vacuum Science Technology A

PLEASE CITE THIS ARTICLE AS DOI: 10.1116/1.5134446

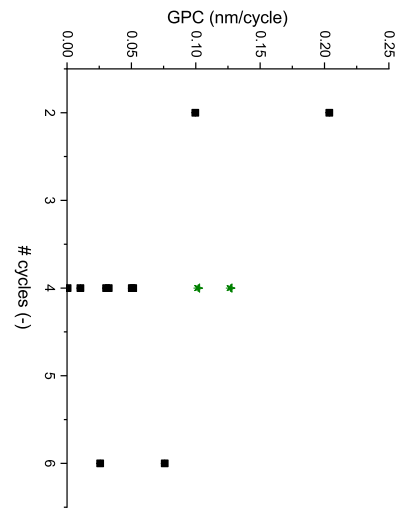

Journal of Vacuum Science Technology A

PLEASE CITE THIS ARTICLE AS DOI: 10.1116/1.5134446

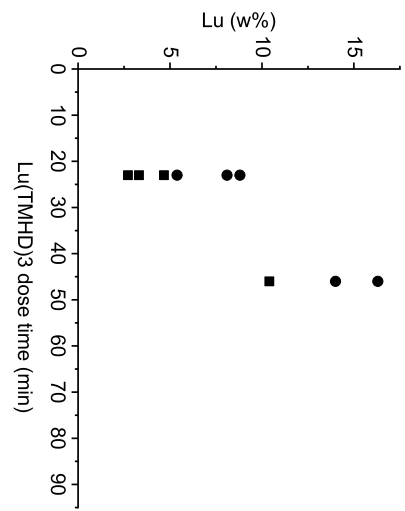

Journal of Vacuum Science Technology A

PLEASE CITE THIS ARTICLE AS DOI: 10.1116/1.5134446